Z. Angew. Math. Phys. 62 (2011), 741–748

0044-2275/11/040741-8
published online July 1, 2011
DOI 10.1007/s00033-011-0144-1

Zeitschrift für angewandte Mathematik und Physik ZAMP

Fully developed laminar slip and no-slip flow in rough microtubes

F. Talay Akyildiz and Dennis A. Siginer

Abstract. The effect of surface roughness on developed laminar flow in microtubes is investigated. The tube boundary is defined by $r = R[1 + \varepsilon \sin(\lambda\theta)]$, with R representing the reference radius and ε and λ the roughness parameters. The momentum equation is solved using Fourier–Galerkin–Tau method with slip at the boundary. A novel semi-analytical method is developed to predict friction factor and pressure drop in corrugated rough microtubes for continuum flow and slip flow that are not restricted to small values of $\varepsilon\lambda$. The analytical solution collapses onto the perturbation solution of Duan and Muzychka (J. Fluids Eng., 130:031102, 2008) for small enough values of $\varepsilon\lambda$.

Mathematics Subject Classification (2000). 76D99 · 35J25 · 65N35 · 41A10.

Keywords. Newtonian fluid · Rough microtubes · Galerkin and Tau method · Semi-analytical solution · Friction factor.

1. Introduction

Advances in microfabrication made it possible to build microchannels with dimensions in the micrometer range. Hence, the mechanics of fluid flow in microchannels emerged as an important research area in view of the many emerging novel industrial applications in biomedical industry, computer chip manufacturing, and separation processes in chemical industry operations among others. A sound understanding of the fluid mechanics and heat transfer issues in microchannels is important for better design of various microfluidic devices. Microchannels are defined as channels whose characteristic dimensions are from 1 μm to 1 mm. Above 1 mm, flow exhibits the same behavior as continuum flows.

In recent years, a large number of papers have reported pressure drop data for laminar fully developed flow of liquids in microchannels with various cross-sections [2]. Rectangular cross-sections have been extensively studied as they are employed in many applications [3]. However, published results are often inconsistent. Some authors report a large deviation from the conventional theories and attribute it to an early onset of laminar to turbulent flow transition or surface phenomena such as surface roughness, electrokinetic forces, viscous heating effects, and microcirculation near the wall [4]. Several theories and models have been proposed to explain the observed deviations, but an indisputable conclusion has not yet been reached.

Because of difficulties involved in current micromachining technology, microchannel walls typically exhibit some degree of roughness, which plays an important role in microchannel flows. But, it is difficult to characterize it analytically or numerically. It can be characterized using stylus-type surface profilometer, optical measurements, scanning electron microscopy (SEM), atomic force microscopy (ATM), and scanning tunneling microscopy (STM). Obviously, there is a need for a better understanding of the effects of wall roughness on fluid characteristics in microchannels.

The method of conformal mapping can be used for the fully developed flow through corrugated tubes (see for example [5]). But, this approach is limited to the shape of the geometry. A model to predict

the pressure drop of the fully developed laminar continuum flows in rough microtubes has been formulated assuming that the wall roughness can be described by an istropic Gaussian distribution, Bahrami et al. [6]. More recently, the effect of corrugated roughness on fully developed laminar flow in microtubes with slip at the boundary has been investigated by Duan and Muzychka [1]. They used a perturbation method to obtain the approximate solution with the wall corrugation as the perturbation parameter, thus restricting the solution to small values of $\varepsilon\lambda$.

In this work, the corrugated domain is transformed first into a computational domain followed by the use of the Fourier–Galerkin–Tau method to solve the transformed momentum equation for unrestricted large values of $\varepsilon\lambda$. The result of the perturbation analysis of Duan and Muzychka [1] is obtained as a special case of this study for small values of $\varepsilon\lambda$.

2. Formulation of the problem

The steady axial flow of a Newtonian fluid through a straight microtube of a uniform cross-section having a circumference in the form of a slightly distorted circle with a radius given by $R\left[1+\varepsilon f\left(\theta\right)\right]$ is considered. ε and R represent the roughness and the mean radius of the rough microtube. The function $f\left(\theta\right)$of the polar angle θ can be chosen to vary the shape of the boundary. To simplify the roughness problem, a sinusoidal corrugation $f\left(\theta\right)=\sin\left(\lambda\theta\right)$ is adopted where $\lambda=2\pi R/l$ with λ and l representing the wave number and the wavelength of the rough corrugated walls, respectively. The dimensionless momentum balance for the axial velocity w reads as,

$$\frac{1}{r}\frac{\partial}{\partial r}\left(r\frac{\partial w}{\partial r}\right)+\frac{1}{r^2}\frac{\partial^2 w}{\partial\theta^2}=-1. \tag{2.1}$$

The no-slip boundary conditions are given by

$$\begin{aligned} w_r=w_\theta=0 \quad \text{at} \quad r=0 \\ w=0 \quad \text{at} \quad r=1+\varepsilon\sin\left(\lambda\theta\right) \end{aligned} \tag{2.2}$$

All variables in these equations are dimensionless; the scale factors $\left[R^2\left(-dp/dz\right)/\mu\right]$ and R are used to non-dimensionalize w and r, respectively. Note that Spectral Fourier–Galerkin method can be used to solve the above problem, but this method cannot be used for the slip flow that is the subject of the next section.

2.1. Slip flow

In the past two decades, the rapid development of microelectromechanic systems (MEMS) and microchemical systems has brought up great interest in studying flow and heat transfer in micro-scale [7]. A sound understanding of the characteristics of slip flow in microchannels in particular in the context of gas flows is becoming increasingly important. The Knudsen number Kn is used to classify gas flow in microchannels in four distinct flow regimes: continuum flow regime ($Kn<0.001$), slip flow regime ($0.001<Kn<0.1$), transition flow regime ($0.1<Kn<10$), and free molecular flow regime ($Kn>10$). The boundary conditions in this case are given by

$$\begin{aligned} &w_r=w_\theta=0 \quad \text{at} \quad r=0, \\ &w=-2Kn\frac{2-\sigma}{\sigma}\frac{\partial w}{\partial \boldsymbol{n}} \qquad r=1+\varepsilon\sin\left(\lambda\theta\right), \qquad Kn=\frac{\lambda_f}{2R} \end{aligned} \tag{2.3}$$

where λ_f is the molecular mean free path and σ denotes the tangential momentum accommodation coefficient usually assumed to be between 0.87 and 1 [7] with $\boldsymbol{n}$ representing the normal vector to the boundary.

2.2. Coordinate transformation

The independent variables in the physical plane (r, θ) are expressed in terms of a new set of independent variables in the computational plane (ζ, t) to map the corrugated microtube domain into a circular cross-section,

$$r = \zeta\left(1 + \sin\left(t\right)\right), \qquad \theta = \frac{t}{\lambda} \tag{2.4}$$

With this transformation, governing Eq. (2.1) in the computational domain takes the following form,

$$\left(g\left(t\right)^2 + \left(\lambda\partial_t g\left(t\right)\right)^2\right)\zeta^2\frac{\partial^2 w}{\partial\zeta^2} - 2g\left(t\right)\partial_t g\left(t\right)\zeta\lambda^2\frac{\partial^2 w}{\partial\zeta\partial t} + \left(g\left(t\right)^2 + 2\left(\partial_t g\left(t\right)\right)^2 - g\left(t\right)\partial_t^2 g\left(t\right)\right)$$
$$\times\lambda^2\zeta\frac{\partial \mathrm{w}}{\partial\zeta} + g\left(t\right)^2\lambda^2\frac{\partial^2 w}{\partial t^2} = -g\left(t\right)^4\zeta^2 \tag{2.5}$$

The local normal gradient at the wall in the transformed computational domain is expressed as

$$\frac{\partial w}{\partial \boldsymbol{n}} = \left(-1 + \frac{\zeta\partial_t g\left(t\right)}{\sqrt{\frac{1}{\lambda^2} + \zeta^2\left(\partial_t g\left(t\right)\right)^2}}\right)\lambda\frac{\partial w}{\partial t} + \frac{\lambda}{g\left(t\right)}\left(\frac{\zeta\partial_t g\left(t\right)}{-\sqrt{\frac{1}{\lambda^2} + \zeta^2\left(\partial_t g\left(t\right)\right)^2}}\right)\frac{\partial w}{\partial\zeta} \tag{2.6}$$
$$g(t) = 1 + \varepsilon\sin(t).$$

As the Fourier–Galerkin method cannot be used to solve the slip flow, a Fourier–Galerkin–Tau method is developed below to solve the problem.

3. Fourier–Galerkin spectral and Tau method

$\{e_k\left(t\right), k \in \mathbb{N}\} = \left\{\frac{1}{\sqrt{2\pi}}e^{ikt}, k \in \mathbb{N}\right\}$ is chosen to be an orthonormal basis of the Hilbert spaces $\mathbb{L}_0^2\left[0, 2\pi\right]$. The subspaces of these Hilbert spaces are spanned by $S_N = \left\{\frac{1}{\sqrt{2\pi}}e^{ikt}, 0 \le k \le N\right\}$. Then, Fourier–Galerkin approximation of (2.5) requires finding functions w_N from $[0, 2\pi] \in S_N$ that satisfy

$$\left(\left(g(t)^2 + \left(\lambda\partial_t g(t)\right)^2\right)\zeta^2\partial_\zeta^2 w_N - 2g(t)\partial_t g(t)\zeta\lambda^2\partial_{\zeta t}^2 w_N + \left(g(t)^2 + 2\left(\partial_t g(t)\right)^2 - g(t)\partial_t^2 g(t)\right)\lambda^2\zeta\partial_\zeta w_N\right.$$
$$\left. + g(t)^2\lambda^2\partial_t^2 w_N + g(t)^4\zeta^2, \varphi\right) = 0 \tag{3.1}$$

with $\varphi \in S_N$. For each ζ, $w_N\left(\zeta, .\right)$ have the following form with superscripts c and s indicating coefficients of the *cos* and *sin* terms, respectively.

$$w_N(\zeta, t) = \frac{\widehat{w}_N^c(\zeta, 0)}{2} + \sum_{k=1}^{N}\widehat{w}_N^s(\zeta, k)\sin(kt) + \widehat{w}_N^c(\zeta, k)\cos(kt) \tag{3.2}$$

with $\varphi = \sin\left(kt\right), 1 \le k \le N - l$ and $\cos\left(kt\right), 0 \le k \le N - l$, the following system of equations for the coefficients of $\widehat{w}_N^s$ and $\widehat{w}_N^c$ are obtained (first few terms):
For $\widehat{w}_N^c\left(0, t\right)$:

$$\partial_\zeta^2\widehat{w}_N^c(\zeta, 0)\left(-4 - 2\varepsilon^2 - 2\varepsilon^2\lambda^2\right) - 8\varepsilon\partial_\zeta^2\widehat{w}_N^s(\zeta, 1) + \left(2\varepsilon^2 - 2\varepsilon^2\lambda^2\right)\zeta\partial_\zeta^2 w_N^c(\zeta, 1) + \cdots = 0 \tag{3.3}$$

For $\widehat{w}_N^c\left(\zeta, 1\right)$:

$$-\partial_\zeta^2\widehat{w}_N^c\left(\zeta, 1\right)\left(4 + \varepsilon^2 + 3\varepsilon^2\lambda^2\right) - 4\varepsilon\partial_\zeta^2\widehat{w}_N^s\left(\zeta, 2\right) + \varepsilon^2\varepsilon\partial_\zeta^2\widehat{w}_N^c\left(\zeta, 3\right) + 3\varepsilon^2\lambda^2\partial_\zeta\widehat{w}_N^c\left(\zeta, 1\right) + \cdots = 0 \tag{3.4}$$

For $\widehat{w}_N^s(\zeta, 1)$:

$$\partial_\zeta^2 w_N^s(\zeta, 1)\left(4 + \varepsilon^2\lambda^2 + 3\varepsilon^2\right) - 4\varepsilon\partial_\zeta^2 w_N^c(\zeta, 2) + \left(\varepsilon^2\lambda^2 - \varepsilon^2\right)\partial_\zeta^2 w_N^s(\zeta, 1) + \varepsilon^2\lambda^2\partial_\zeta^2 w_N^s(\zeta, 3) + \cdots = 0 \tag{3.5}$$

In this work, polynomial approximations are used for $w_N^c(\zeta,0), w_N^s(\zeta,k), 1 \le k \le N$, and $w_N^c(\zeta,k)$, $1 \le k \le N$. The selection of trial functions and the solution method used are different for no-slip flow and slip flow because of the boundary conditions.

(i) No-slip flow

Trial functions are constructed in the following way to satisfy boundary conditions,

$$\bigwedge_i(\zeta) = \left(1-\zeta^2\right)\zeta^{2i}, \quad i = 0,1,\ldots,n \tag{3.6}$$

Hence, in terms of trial functions, $w_N^c(\zeta,0), w_N^s(\zeta,k)$, and $w_N^c(\zeta,k), 1 \le k \le N$ can be rewritten as

$$w_N^c(\zeta,0) = \sum_{j=0}^{N} a[0,j](1-\zeta^2)\zeta^{2j}, \quad w_N^c(\zeta,k) = \sum_{j=0}^{N} a[i,j](1-\zeta^2)\zeta^{2j}$$

$$w_N^s(\zeta,k) = \sum_{j=0}^{N} b[i,j]\left(1-\zeta^2\right)\zeta^{2j}, \quad i = 1,\ldots,N$$

$a[0,j], a[i,j], b[i,j]$ are unknown coefficients to be determined. Substituting these expressions into (3.2), we derive

$$w_N(\zeta,t) = \sum_{j=0}^{N} a[0,j]\left(1-\zeta^2\right)\zeta^{2j} + \sum_{i,j=1}^{N}\left(a[i,j]\cos(it) + b[i,j]\sin(it)\right)\left(1-\zeta^2\right)\zeta^{2j} \tag{3.7}$$

Galerkin spectral method can now be used to find the unknown parameters. Note that the following boundary conditions are automatically satisfied

$$\begin{aligned} w_\zeta = w_t = 0 \quad &\text{at } \zeta = 0 \\ w = 0 \quad &\text{at } \zeta = 1 \end{aligned} \tag{3.8}$$

(ii) Slip flow

Trial functions are chosen as

$$\bigwedge_i(\zeta) = \zeta^{2i}, \quad i = 0,1,\ldots,n \tag{3.9}$$

First boundary conditions in (2.3) for slip flow are automatically satisfied, and $w_N(\zeta,t)$ together with boundary conditions can be written in terms of the trial functions as

$$\begin{aligned} w_N(\zeta,t) = &\sum_{j=0}^{N} a[0,j]\zeta^{2j} + \sum_{i,j=1}^{N-1}\left(a[i,j]\cos(it) + b[i,j]\sin(it)\right)\zeta^{2j+2} \\ &+ a[N-1,N]\cos((N-1)t)\zeta^{2N+2} + a[N,N-1]\cos(Nt)\zeta^{2N} \\ &+ b[N-1,N]\sin((N-1)t)\zeta^{2N+2} + a[N,N-1]\sin(Nt)\zeta^{2N} \end{aligned} \tag{3.10}$$

$$\partial_\zeta w_N = \partial_t w_N = 0 \quad \text{at} \quad \zeta = 0 \tag{3.11}$$

$$\begin{aligned} 2Kn\frac{2-\sigma}{\sigma}&\left(\left(-1 + \frac{\partial_t g(t)}{\sqrt{\frac{1}{\lambda^2} + \left(\partial_t g(t)\right)^2}}\right)\lambda\partial_t w_N(1,t)\right. \\ &\left. + \frac{\lambda}{g(t)}\left(\left(\partial_t g(t) - \sqrt{\frac{1}{\lambda^2} + \left(\partial_t g(t)\right)^2}\right)\zeta w_N(1,t)\right)\right) + w_N(1,t) = 0 \end{aligned} \tag{3.12}$$

Note that the trial function (3.9) does not satisfy boundary condition (3.12) for slip flow. Thus, it is necessary to have weighted residual conditions for both the PDE and second boundary condition. Substituting this into (3.10) and using the method of spectral Tau, we obtain $N^2 - l$ equations with N^2 unknowns; the

remaining l equations comes from the application of weighted residual method to the second boundary condition (3.12),

$$\int_0^{2\pi} \left(\left(\left(-1 + \frac{\partial_t g\,(t)}{\sqrt{\frac{1}{\lambda^2} + (\partial_t g\,(t))^2}} \right) \lambda \partial_t w_N\,(1,t) + \frac{\lambda}{g\,(t)} \left(\partial_t g\,(t) - \sqrt{\frac{1}{\lambda^2} + (\partial_t g\,(t))^2} \right) \partial_\zeta w_N\,(1,t) \right) \times 2Kn \frac{2-\sigma}{\sigma} + w_N(1,t) \right) \varphi dt = 0 \tag{3.13}$$

$$\varphi = \sin kt, N - l \le k \le N - \frac{l}{2} \quad \text{and} \quad \cos kt, N - l/2 \le k \le N - l.$$

As (3.13) cannot be integrated exactly, the quadrature method is used to evaluate the integral numerically. Thus, a system of N^2 equations with N^2 unknowns is obtained. This is the essence of the spectral Tau approximation. The resulting matrix is checked carefully for each run of the program for different values of the parameters involved in the non-singular flow problem. It is well known that the solution is unique. Convergence of the solution and the results are discussed in the following section in detail.

The total flow rate is given by

$$Q = \int_0^{2\pi} \int_0^1 w\,(\zeta, t)\, g\,(t)^2\, \mathrm{d}\zeta \mathrm{d}t. \tag{3.14}$$

The ratio $Q^* = Q/Q_{\mathrm{sm}}$ can be readily computed. Q_{sm} is the flow rate for smooth microtubes. Similarly, the effect of wall roughness on the pressure drop $\Delta p^* = \Delta p/\Delta p_{\mathrm{sm}}$ is computed and used in the plots of Figs. 1 and 2. Δp_{sm} is the pressure drop for the smooth microtube and Δp is given by

$$\Delta p = \frac{8Q}{\pi} \tag{3.15}$$

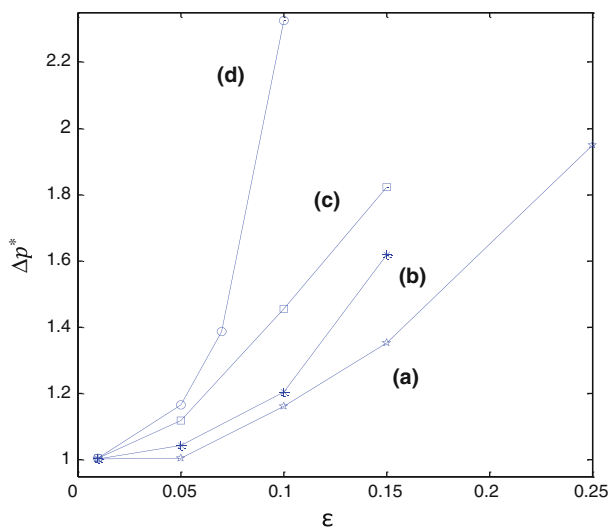

FIG. 1. Effect of relative roughness ε and wave number λ on the pressure drop in microtubes for continuum flow. **a** Galerkin method ($\lambda = 10$), **b** perturbation method ($\lambda = 10$), **c** Galerkin method ($\lambda = 30$), **d** perturbation method ($\lambda = 30$)

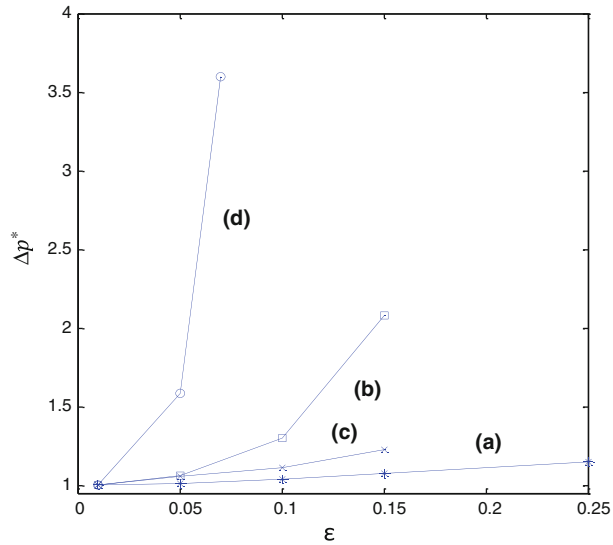

FIG. 2. Effect of relative roughness ε and wave number λ on pressure drop in microtubes for continuum flow for $Kn^* = 0.03$ flow. **a** Galerkin method ($\lambda = 10$), **b** perturbation method ($\lambda = 10$), **c** Galerkin method ($\lambda = 30$), **d** perturbation method ($\lambda = 30$)

The friction factor times Reynolds number fRe can be obtained simply by substituting (3.14) into the definition of fRe with D_h representing the hydraulic radius,

$$fRe = \frac{2\left(\frac{A}{P}\right) D_h A}{Q} \tag{3.16}$$

4. Discussion and conclusion

Both methods give the exact solution for $\varepsilon = \lambda = 0$. The convergence of the methods is checked by increasing the number of terms in (3.7) and (3.10) until the difference between successive solutions is less than 10^{-6} for $\varepsilon = 0.1$ and $\lambda = 3$ for both no-slip and slip flow with $K_n^* = K_n\,(2-\sigma)\,/\sigma = 0.03$. The results are compared with the perturbation solution of Duan and Muzychka [1] in Table 1 in terms of friction factor times Reynolds number fRe.

The perturbation solution agrees with the results of the semi-analytical Fourier–Galerkin–Tau method developed in this paper for small enough $\varepsilon\lambda$. In fact, if $\varepsilon\lambda \leq 1$, the difference between perturbation solution and the semi-analytical Fourier–Galerkin–Tau solution is negligible. Perturbation solution is no longer valid if $\varepsilon\lambda > 1$ as the difference clearly is unacceptable.

TABLE 1. *fRe for developed laminar flow in corrugated microtubes with no-slip for $\lambda = 50$*

ε	$fRe(perturbation)$	$fRe(Galerkin\ method)$
0.01	1.00979	1.00972
0.02	1.03069	1.04036
0.03	1.05822	1.09565
0.04	1.10152	1.18371
0.05	1.1708	1.32013

TABLE 2. *fRe for developed laminar flow in corrugated microtubes with slip for* $\lambda = 50$

ε	$fRe(perturbation)$	$fRe(Tau\ method)$
0.01	1.010831	1.0398
0.02	1.033376	1.1808
0.03	1.056105	1.52569
0.04	1.0756	2.58
0.05	1.0920	23.319

Slip flow results are tabulated in Table 2 for a specific value of λ and several values of ε. The conclusions reached for the no-slip flow on the basis of Table 1 are valid for slip flow as well, that is the perturbation solution of Duan and Muzychka [1] agrees fairly well with the results of the semi-analytical Fourier–Galerkin–Tau method for small enough $\varepsilon\lambda$, and there is an increasingly large discrepancy for $\varepsilon\lambda > 1$. It should be noted that for slip flow the discrepancy between the perturbation and the Galerkin–Tau method results is much larger than the discrepancy for the no-slip flow for the same value of $\varepsilon\lambda$ between the perturbation and the Galerkin methods. In fact for $\varepsilon\lambda = 2.5$, it is an order of magnitude larger. The discrepancy between the perturbation and the Galerkin method in the case of no-slip flow and the Galerkin–Tau method in the case of slip flow grows rapidly with growing $\varepsilon\lambda$, but it grows at a much faster rate in the case of slip flow.

Figure 1 summarizes the comparison for the pressure drop results for two values of λ and several values of ε covering a wide range of these parameters for continuum no-slip flow. In all cases for a given λ and ε, the perturbation solution estimates a pressure drop larger than that predicted by the Fourier–Galerkin solution, even for relatively small values of λ and ε. The discrepancy grows with increasing ε for fixed λ. The larger the λ, the larger becomes the gap between the perturbation and the Fourier–Galerkin solution for the same ε. The gap between the perturbation and the Fourier–Galerkin solution starts opening up earlier that is at smaller and smaller ε with growing λ.

Figure 2 summarizes pressure drop results for slip flow for $Kn = 0.03$ and for the same range of values of λ and ε as in Fig. 1. The qualitative conclusions drawn from Fig. 1 for the case of continuum no-slip flow hold for the slip flow data of Fig. 2 as well with the proviso that agreement between the perturbation solution and the Fourier–Galerkin–Tau method is relatively better for smaller λ and ε. However, for larger values of λ, there is no agreement at all even for very small ε.

References

1. Duan, Z., Muzychka, Y.M.: Effects of corrugated roughness on developed laminar flow in microtubes. J. Fluids Eng. **130**, 031102 (2008)
2. Bahrami, M., Yovanovich, M.M., Culham, J.R.: Pressure drop of fully developed, laminar flow in rough microtubes. J. Fluids Eng. **128**, 632–637 (2006)
3. Wang, X.Q., Yap, C., Mujumdar, A.S.: Effects of two dimensional roughness in flow in microchannel. J. Electron. Packag. **127**, 357–361 (2005)
4. Pfund, D., Rector, D., Shekarriz, A., Popescu, A., Welty, J.: Pressure drop measurements in a microchannel. AIChE J. **46**(8), 1496–1507 (2000)
5. Hu, M.H.: Flow and thermal analysis for mechanically enhanced heat transfer tubes, Ph.D. thesis, State University of New York at Buffalo, New York (1973)
6. Bahrami, M., Yovanovich, M. M., Culham, J. R.: Pressure drop of fully-developed laminar flow in rough microtubes, Proceedings of Micromini, 3rd International Conference on Microchannels and Minichannels, June 13–15, Toronto, Ontario, Canada (2005)
7. Cao, B., Chen, G.W., Yuan, Q.: Fully developed laminar flow and heat transfer in smooth trapezoidal microchannel. Int. Commun. Heat Mass Transf. **32**, 1211–1220 (2005)

F. Talay Akyildiz
Department of Mathematics
Petroleum Institute
Abu Dhabi
UAE
e-mail: fakyildiz@pi.ac.ae

Dennis A. Siginer
Department of Mechanical Engineering and Department of Mathematics
Petroleum Institute
Abu Dhabi
UAE

(Received: June 8, 2010)